

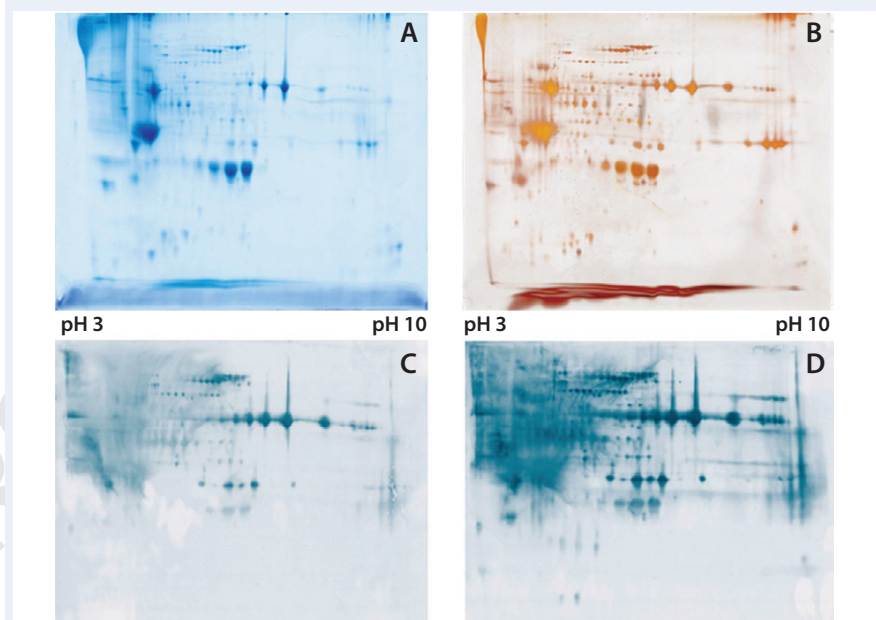
# Development of a Novel Host-Cell Protein Assay

## Supporting the *Physcomitrella patens* Expression System

Paulina Dabrowska-Schlepp, Stefan Sommerschuh, Mathias Knappenberg, Holger Niederkrüger, Nicole Gliese, and Andreas Schaaf

**H**ost-cell proteins (HCPs) constitute an inevitable impurity of biopharmaceutical products originating from recombinant-cell culture. HCPs are a heterogeneous mix of different proteins, their specific characteristics depending on the kind of organism used as an expression platform, on the “destination” of the expressed recombinant product (extra- or intracellular), and on the corresponding purification approach (1–3). Contamination of a final drug substance with residual HCPs could lead to immunogenic reactions in some patients who receive the drug product (DP). So a reliable method for identifying — and quantifying — HCPs is an integral component of biopharmaceutical purification processes and quality specification of a final drug product.

**Figure 1:** (A) Two-dimensional (2D) sodium-dodecyl sulfate polyacrylamide gel electrophoresis (SDS-PAGE) total protein Coomassie stain of the *Physcomitrella patens* HCP antigen mix, 600 µg protein per gel; (B) 2D SDS-PAGE total protein silver stain of the *P. patens* HCP antigen mix, 300 µg protein per gel; (C) quality control testing of the total antiserum pool by 2D Western blot, 300 µg protein per gel; (D) quality control testing of the capture antibody by 2D Western blot, 300 µg protein per gel



**PRODUCT FOCUS:** ANTIBODIES AND OTHER PROTEINS

**PROCESS FOCUS:** DOWNSTREAM PROCESSING

**WHO SHOULD READ:** QA/QC, ANALYTICAL, MANUFACTURING, AND PROCESS DEVELOPMENT

**KEYWORDS:** IMMUNOASSAYS, PLANT CELL CULTURE, WESTERN BLOTting, AFFINITY CHROMATOGRAPHY, BRADFORD ASSAY

**LEVEL:** INTERMEDIATE

Generic protein-detection methods such as total protein stains are insufficiently sensitive, especially in the presence of a great excess of recombinant product. Tscheliessnig, et al. overviewed methods for HCP detection, classifying them into immunospecific (immunoassays, Western blotting) and nonspecific (electrophoresis and MS-based) technologies (3). In most cases, enzyme-linked immunosorbent assays (ELISAs) have become the method of

choice for HCP measurements (1, 2, 4, 5). They are based on polyclonal anti-HCP antisera generated with a representative HCP mix originating from a null cell-line culture.

Because most expression systems are based on bacterial and mammalian cells, a broad range of “generic” HCP assays are commercially available for such platforms. However, a growing amount of evidence suggests a lack of efficiency in HCP detection for those assays (3, 5), so a fine tuning of such

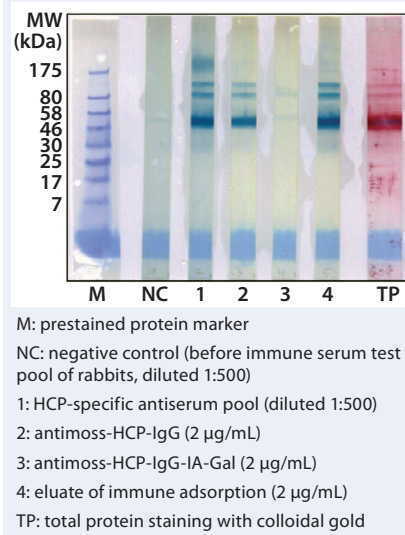
ELISAs probably is necessary (6). Because plant-based expression systems such as *Physcomitrella patens* have emerged only recently as an alternative to established recombinant-protein production platforms, corresponding plant-specific solutions for HCP quantification are needed. Here also, a specific immunoassay (ELISA) seems to be the method of choice (7, 8), although use of specifically tailored mass-spectrometric (MS) techniques has been reported. Nevertheless, development of a plant-cell-specific HCP assay (combined with identification of the most potent plant HCPs) has yet to be described.

Greenovation Biotech GmbH is a German biopharmaceutical company developing treatments for rare diseases using its proprietary BryoTechnology manufacturing platform based on moss (*Physcomitrella patens*) as an expression platform. This plant-based system strictly eliminates animal-derived media and strain components, making it free of zoonotic pathogens. Moss-expressed biopharmaceuticals meet high quality standards because plants can perform complex posttranslational modifications — and specifically, the moss is highly accessible to stable genetic engineering. The system thus allows for product-tailored solutions that could ameliorate a number of therapeutic outcomes (9, 10).

In 2014, Greenovation completed the first good manufacturing practice (GMP)-compliant production of its leading clinical candidate: human alpha-galactosidase ( $\alpha$ Gal) for treatment of Fabry disease. To meet requirements for release of DP material to be used in the phase 1 clinical trial in Germany, it was necessary to develop a *P. patens*-specific HCP immunoassay in collaboration with BioGenes GmbH.

Although not in the main scope of industry-driven research, identity and composition of a species-specific HCP cocktail can be of interest for better understanding of this expression system. Ultimately this could help improve it over time (e.g., through targeted development of specific

**Figure 2:** Western blot cross-reactivity after antibody immune adsorption against alpha galactosidase, 500 ng ( $\alpha$ Gal) protein per strip; MW of moss- $\alpha$ Gal = 46 kDa



knock-out strains). Here, we report our development of a *P. patens*-specific HCP ELISA, which we used subsequently for quantification of HCPs during GMP-compliant production of moss-made  $\alpha$ Gal. Moreover, we used 2D gel electrophoresis and LC-MS-MS analysis to identify major HCPs present in the supernatant of *P. patens* culture.

#### ANTIGEN PREPARATION

Our representative HCP preparation came from a “mock” culture of the fucose/xylose double-knockout mutant (FT3/XT-ko) used as a background for most of Greenovation’s producer strains (11–13). In that strain, moss genes for plant-type fucosyl- and xylosyl-transferases have been deactivated by a homologous recombination technique, leading to humanized N-glycans (11). Because the HCP amounts are low in supernatant from our standardized fermentation process with *P. patens*, we needed a 100-L cultivation scale to obtain sufficient amounts of antigens for subsequent rabbit immunization.

The FT3/XT-ko strain was cultured for four weeks in a 100-L (200-L nominal volume) disposable Cellbag 200 bag (GE Healthcare) placed in a BioWave 200 SPS rocking bioreactor (GE Healthcare). The

main culture parameters — medium, time, gas exchange, light intensity, and addition of osmotic active substances leading to protein secretion — corresponded to standard conditions used for manufacturing of most protein products at Greenovation. We determined the supernatant HCP concentration using a standard Bradford assay. At the end of cultivation (28 days), that concentration was 13 mg/L.

Moss biomass reached 4.5 g/L dry weight and was subsequently separated from the supernatant with the following filtration cascade:

- moss harvest through cake filtration in a customized PP filtration housing (14) equipped with a 8.0- to 20.0- $\mu$ m Seitz K900 320D filter (Pall GmbH)
- depth filtration through two nominal exclusion sizes: Supracap 100 NP6P7001 and Supracap 100 NP8P0501 (Pall)
- 0.45- $\mu$ m and 0.2- $\mu$ m Sartopore 2 5445307H9 sterile filtration (Sartorius Stedim Biotech).

We divided the combined sterile filtrate into two batches, concentrating both and rebuffing them with tangential-flow filtration (TFF) on a Centramate 500S TFF cross-flow filter (Pall). Equipped with a 10-kDa cut-off DC010T12 T-Series TFF cassette with Delta regenerated cellulose membrane (Pall), it delivered

- 550 mL HCP antigen mix with ~370 mg/L protein concentration in Tris-based buffer, subsequently used for rabbit immunization and characterization of the HCP antigen mix
- 1.9 L HCP antigen mix with ~47 mg/L protein in 0.01 M phosphate-buffered saline (PBS) solution, used for preparation of an affinity column for subsequent purification of antibodies from rabbit antisera.

To maximize the amount of antigen for rabbit immunization in one injection round, we further concentrated the 550-mL HCP antigen mix with ultrafiltration using a 10-kDa cut-off Amicon ultrafiltration cell (EMD Millipore)

to a final concentration of ~890 mg/L. Again, we determined the protein content of antigen pools using a standard Bradford assay.

### DEVELOPMENT OF ANTI-HCP ANTIBODIES

We injected the concentrated HCP antigen mix into five rabbits, repeating those immunization injections 11 times over the course of six months to secure broader antigen recognition (5, 15). We bled the animals eight times, including a terminal bleeding. Altogether, we collected a 1.1-L antiserum pool from all animal bleedings and used an aliquot of 200 mL for affinity purification against the HCP antigen mix. We prepared an affinity matrix according to manufacturer's instructions (GE Healthcare) by coupling ~25 mg of the HCP antigen mix onto Bromocyan-activated Sepharose chromatography media. Subsequently, we affinity-purified an antiserum volume of 200 mL to generate capture antibodies (antimoss-HCP-IgG at a concentration of 2.14 mg/mL).

A 13-mg aliquot of the isolated capture antibody served as starting material for preparation of detector antibodies. We dialyzed it against PBS and conjugated it with biotin to prepare detector antibodies that in

turn would react with the enzyme conjugate (streptavidin-conjugated peroxidase). For biotin conjugation of the antibodies, we used a 40-fold molar excess of the biotinylation reagent (biotinamidohexanoic acid N-hydroxysuccinimide ester from Sigma-Aldrich) over immunoglobulin G (IgG). Then we removed the biotinylation reagent by dialysis in Tris-buffered saline and mixed the resulting antimoss-HCP-IgG-Biotin (0.79 mg/mL) with  $\text{NaN}_3$  for preservation.

To check the quality of our generated antibodies and ensure their recognition and coverage of *P. patens* HCP mix, we performed two-dimensional (2D) analyses and compared the total protein pattern of the HCP antigen mix visualized with Coomassie and silver staining (Figures 1A and B) with HCP-specific Western blot patterns, using both the antiserum pool and the affinity-purified capture antibodies. As Figures 1c and 1d show, clearly stained HCP-specific Western blot signals appeared over the whole molecular weight range in both cases of 2D Western blotting. Those signals agreed well with the in-gel stained total protein patterns (Figure 1A and B), particularly for the capture antibody as visually estimated (Figure

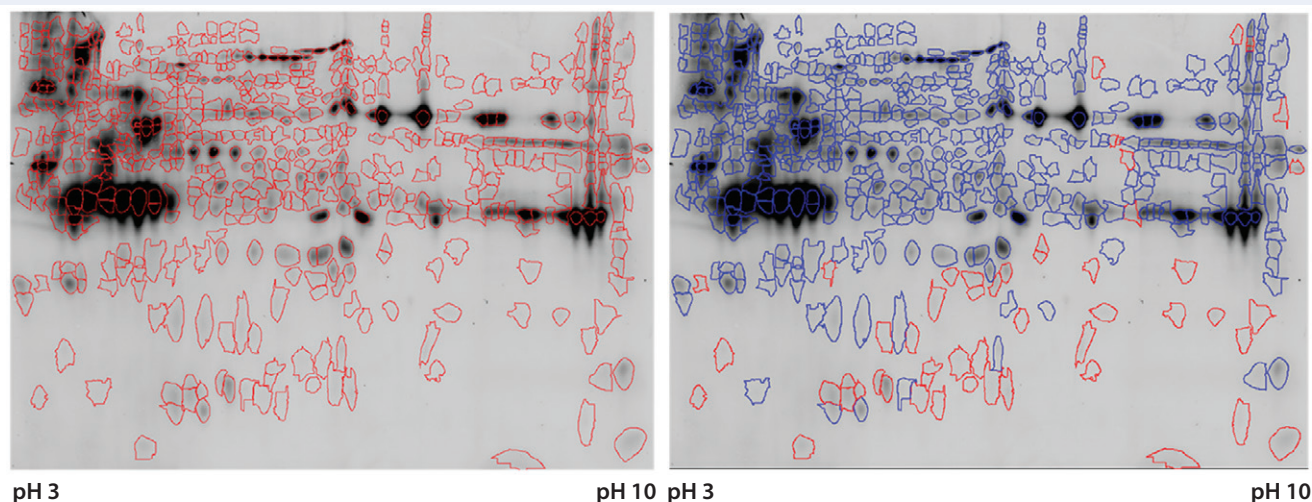
1d). Differences in the staining intensity between the antiserum pool and capture antibody might be due to different absolute antibody concentrations in the purified antibody solution and the unpurified antiserum. In general, we were able to generate and isolate an appropriate set of antibodies that sufficiently recognize a *P. patens* HCP antigen mix.

### DEVELOPMENT AND EVALUATION OF HCP SANDWICH ELISA

For development of a sandwich ELISA, we optimized several parameters: concentration of the capture antibody, concentration of the detector antibody, and the incubation times with both antigen and detector antibodies. A suitable HCP master standard was prepared from the HCP antigen mix material. We set the preliminary working range of the assay to 0.1–5.0 ng/mL and obtained an acceptable intraassay precision with a coefficient of variance (CV) <4%. Those values came from optimized assay conditions, and we verified them in our validation study with samples originating from the actual moss culture as described below.

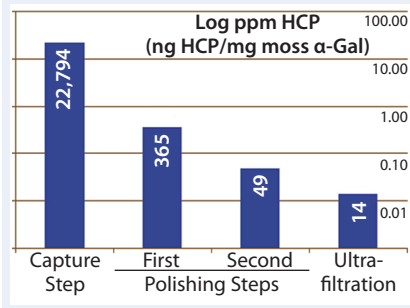
### Optimization, Implementation, and Validation of the HCP Assay in GMP Compliant Production of Moss-Made

**Figure 3:** Cy5 and Cy3 scan of 2D fluorescence Western blot with electronic spot detection: (LEFT) 2D fluorescence Western moss-HCP1-Cy5 image (580 detected protein spots marked red), 50  $\mu\text{g}$  protein per gel; (RIGHT) moss-HCP1-Cy5 protein pattern compared with antimoss-HCP-IgG-IA-Gal immunodetection pattern detected with antirabbit-IgG-Cy3 conjugate (527 detected spots framed blue, undetected spots remain red-framed), middle-intensity exportation of fluorescence scan (PMT scanning settings Cy5 525 V and Cy3 425 V).



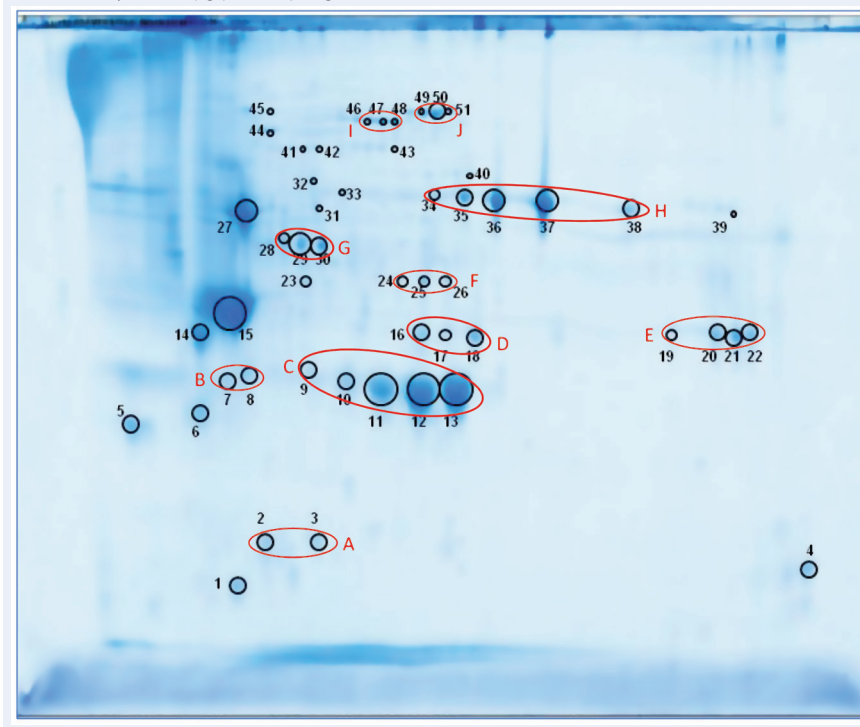
ImageMaster 2D Platinum software version 7.0 was used for electronic determination of HCP coverage in 2D fluorescence Western blots. At first, the antigen-Cy5 image was analyzed with a spot-detection tool (580 spots, left), and then the detected total protein spot pattern was propagated to the Cy3 HCP-specific immunostaining image. Intensity of the Cy3 signal behind a discrete protein spot was used to define a spot as antibody-detected or not (527 immuno-detected spots, right). HCP coverage of antibodies was calculated (percentage compared with the Cy5 total protein spot count as 100% value) at 90.8%.

**Figure 4:** Host-cell protein amounts (ng HCP per mg moss- $\alpha$ Gal) at different steps in downstream processing of the moss  $\alpha$ Gal from 100-L GMP-compliant production culture



**Alpha-Galactosidase:** We analyzed a set of samples from the culture and purification of moss  $\alpha$ Gal in a feasibility test with the developed HCP ELISA (16). We observed minor cross-reactivity between a small part of the HCP-specific antibodies and the recombinantly expressed  $\alpha$ Gal and confirmed this with a 1D Western blot (Figure 2). To exclude unspecific binding phenomena from our Western blot, we additionally carried out ELISA inhibition tests that confirmed the presumed cross-reactivity under near-native conditions in contrast to the Western blot method (data not shown). In such inhibition tests, samples are preincubated with potentially cross-reacting antibodies in excess over residual HCP but not in excess over the drug product to inhibit fully the HCP-derived signals. If any

**Figure 5:** 2D SDS-PAGE total protein Coomassie stain of *P. patens* HCP antigen mix with 51 protein spots, which were identified using liquid chromatography with tandem mass spectrometry (LC-MS-MS) analysis; 600  $\mu$ g protein per gel



remaining ELISA reactivity is then observed in samples compared with a suitable buffer control, then that indicates product cross-reactivity with capture and detector antibodies used in the assay.

Although such cross-reactivity between HCP-specific antibodies and drug substance is rare, it might occur in some HCP immunization trials.

However, cross-reacting antibodies can be depleted by immune adsorption of capture antibodies against the drug substance. So part of the HCP-specific capture antibodies were immune-adsorbed by passage through an affinity matrix loaded with purified moss-derived  $\alpha$ Gal. The newly obtained pool of anti-HCP antibodies (antimoss-HCP-IgG-IA-Gal)

**Table 1:** Summary of preliminary assay validation; determination of LoD and LoQ through spike experiments is planned, along with full validation of the assay, before upcoming production of material for phase 2 clinical trials.

Parameter	Experimental Setup	Acceptance Criteria	Result
Specificity	Spike experiments with solutions of purified drug substance and samples from process steps (five independent samples, each measured in triplicate)	Spike recovery for each of spiked sample must be 80–120%.	Spike recovery was 88–96%.
Linearity	Two separate dilution series (5.0, 3.0, 2.0, 1.0, 0.5, 0.2 and 0.1 ng/mL) each measured in triplicate, analyzed, and calculated concentrations plotted against expected concentrations	Mean recovery for each dilution should be 80–120%.  Coefficient of determination of linear fit of the plot should be $r^2 \geq 0.99$ .	Recoveries for each dilution were in the range of 93–100%.  The coefficient of determination is $r^2 \geq 0.99$ .
Repeatability	Analysis of three samples with HCP concentrations covering the specified range, each in triplicate; %CV calculated for nine concentrations; repeatability across the range supported by the recovery tested for linearity	The %CV of all nine concentrations should be $\leq 15\%$ .	%CV ( $n = 9$ ) based on all nine concentrations was 6.1%.
Range	Tested with linearity	The range must be at least 0.2–5.0 ng/mL.	The range is 0.1–5.0 ng/mL.
Accuracy	Inferred from suitable specificity, linearity, and repeatability	Suitable specificity, linearity and repeatability.	Suitable specificity, linearity and repeatability shown.
Limit of detection (LoD)	LoD interpolated from assay standard curve (mean absorbance of the blank + $3.3 \times$ SD of the blank)	NA	0.06 ng/mL
Limit of quantitation (LoQ)	LoD interpolated from assay standard curve (mean absorbance of the blank + $10 \times$ SD of the blank)	NA	0.08 ng/mL

**Table 2:** Results of MASCOT searches using MS-MS spectra against *P. patens*-specific database version 1.6 (www.cosmos.org)

Group	Spot	GenBank Number	Predicted Mass	Protein Score	Peptide Hits*	Description**
A	1	EDQ74503	20,708 Da	1,057	1	no functional description
	2	EDQ75769	15,292 Da	82	2	translational inhibitor protein
		EDQ78993	13,694 Da	69	2	thioredoxin h
	3	EDQ78993	13,694 Da	366	3	thioredoxin h
	4	EDQ76689	13,399 Da	251	4	no functional description
B	5	EDQ62869	12,361 Da	79	1	rhicadhesin receptor
	6	CAH58720	25,465 Da	77	1	outer membrane lipoprotein BLC (lipocalin)
		CAH58720	25,465 Da	1,369	4	outer membrane lipoprotein BLC (lipocalin)
7	CAH58715	32,397 Da	257	7	xyloglucan endotransglucosylase hydrolase protein 9	
	CAH58715	32,397 Da	1,310	7	xyloglucan endotransglucosylase hydrolase protein 9	
C	9	EDQ62820	24,551 Da	252	6	germin-like protein (Cupin domain containing)
	10	EDQ62820	24,551 Da	353	7	germin-like protein (Cupin domain containing)
	11	EDQ62820	24,551 Da	721	10	germin-like protein (Cupin domain containing)
	12	EDQ62820	24,551 Da	492	9	germin-like protein (Cupin domain containing)
	13	EDQ62820	24,551 Da	589	11	germin-like protein (Cupin domain containing)
D	14	CAH58717	31,926 Da	498	6	chitinase
	15	CAH58716	32,397 Da	1,837	11	xyloglucan endotransglucosylase hydrolase protein 9
	16	EDQ51179	31,371 Da	683	3	spherulin-4 precursor
E	17	EDQ51179	31,371 Da	341	3	spherulin-4 precursor
	18	EDQ51179	31,371 Da	301	3	spherulin-4 precursor
F	19	EDQ69736	32,679 Da	2,021	15	concanavalin A-like lectin protein
	20	EDQ69736	32,679 Da	2,030	13	concanavalin A-like lectin protein
	21	EDQ69736	32,679 Da	785	16	concanavalin A-like lectin protein
	22	EDQ69736	32,679 Da	2,343	15	concanavalin A-like lectin protein
	23	EDQ49699	42,442 Da	208	7	fructose-bisphosphate aldolase, chloroplast precursor (ALDP)
G	24	EDQ64292	42,280 Da	565	15	ferredoxin-nadp <sup>+</sup> reductase-like protein
	25	EDQ64292	42,280 Da	311	12	ferredoxin-nadp <sup>+</sup> reductase-like protein
	26	EDQ64292	42,280 Da	608	20	ferredoxin-nadp <sup>+</sup> reductase-like protein
H	27	EDQ72236	57,062 Da	1,514	15	glyoxal oxidase
	28	EDQ56868	40,606 Da	799	16	pectin methylesterase
	29	EDQ56868	40,606 Da	654	14	pectin methylesterase
	30	EDQ56868	40,606 Da	795	16	pectin methylesterase
	31	EDQ63243	61,054 Da	973	18	glyoxal oxidase
	32	EDQ51428	60,796 Da	818	25	glyoxal oxidase
I	33	EDQ60297	57,651 Da	705	14	glyoxal oxidase
	34	CAH58716	46,684 Da	693	23	alpha-L-fucosidase 2 (lipase GDSL)
	35	CAH58716	46,684 Da	1,863	25	alpha-L-fucosidase 2 (lipase GDSL)
	36	CAH58716	46,684 Da	2,218	25	alpha-L-fucosidase 2 (lipase GDSL)
	37	CAH58716	46,684 Da	3,009	30	alpha-L-fucosidase 2 (lipase GDSL)
	38	CAH58716	46,684 Da	1,276	24	alpha-L-fucosidase 2 (lipase GDSL)
	39	EDQ60560	46,533 Da	735	19	alpha-L-fucosidase 2 (lipase GDSL)
	40	EDQ67270	53,190 Da	710	21	mtLPD2 (lipoamide dehydrogenase 2) ATP binding dihydrolipoyl dehydrogenase
	41	EDQ73806	85,699 Da	760	9	subtilase family protein
	42	EDQ73806	85,699 Da	1,401	11	subtilase family protein
	43	EDQ73806	85,699 Da	627	15	subtilase family protein
	44	EDQ57075	54,260 Da	1,076	13	subtilisin proteinase-like
	45	EDQ75576	102,109 Da	282	9	nodulation receptor kinase
J	EDQ57075	54,260 Da	208	8	subtilisin proteinase-like	
	46	EDQ73806	85,699 Da	2,134	18	subtilase family protein
	47	EDQ73806	85,699 Da	1,934	18	subtilase family protein
K	48	EDQ73807	85,699 Da	2,197	18	subtilase family protein
	49	EDQ82172	86,414 Da	394	11	subtilase family protein
	50	EDQ82172	86,414 Da	336	9	subtilase family protein
51	EDQ82172	86,414 Da	253	8	subtilase family protein	

\* number of peptides matching best hit in the MASCOT search

\*\* description of protein in the database

subsequently tested negative for cross-reactivity with  $\alpha$ Gal by Western blotting (Figure 2) and ELISA, as described above. Additionally, we again evaluated coverage of *P. patens* HCP mix with our new antimoss-HCP-IgG-IA-Gal pool using 2D difference gel electrophoresis (DIGE) fluorescence Western blotting. We compared the 2D protein pattern of the Cy5-labeled HCP antigen with the HCP-specific Western blot pattern, in which the antimoss-HCP-IgG-IA-Gal was used together with secondary antirabbit-IgG-Cy3 conjugate. Our determination of HCP coverage by image analysis (using ImageMaster 2D Platinum version 7.0 and ImageQuantTL software from GE Healthcare) amounted to 90.8% (Figure 3 A and B).

Next we implemented our optimized assay as an in-process control in downstream purification of the moss  $\alpha$ Gal. Figure 4 illustrates the gradual depletion of HCP levels along each purification step, with a 14 ppm in the final drug substance. That value complies well with HCP levels of <100 ng/mg accepted by regulators for drug substances (1).

At this stage, our assay has been partially validated in terms of specificity, linearity, limits of detection and quantitation (LoD, LoQ), range, repeatability, and accuracy. Table 1 summarizes our validation results.

## CHARACTERIZATION OF THE HCP ANTIGEN MIX

We separated the concentrated HCP antigen mix by 2D-PAGE followed by Coomassie staining to deliver a widespread protein pattern over the whole molecular-weight range. We aimed to further characterize the host-cell proteome of *P. patens* (FT3/XT-ko strain) generated under Greenovation's standard culture conditions. Therefore, we chose 51 of the most prominent protein spots (Figure 5) and identified them by analyzing the tryptic peptides with nanoLC-MS-MS. Subsequently, we subjected the obtained spectra to searches in an online *P. patens*-specific database (www.cosmoss.org)

using the MASCOT search algorithm (17).

Table 2 summarizes the best protein hits for each spot. Clearly visible from the 2D gel protein pattern, 33 of 51 protein spots cluster into 10 groups (Table 2, A–J). Those proteins with different isoelectric points but similar molecular weights may represent isoforms of the same protein. Identification results support that observation, with the highest scores obtained for protein spots belonging to the same group in almost all cases (groups B–J) and assigned to the same protein. Identification of the HCP mix revealed the following groups:

- enzymes with proven function in modification of the *P. patens* cell wall — xyloglucan endotransglucosylase hydrolase (group B) and pectin methylesterase (18, 19) (group G)
- proteins implicated in resistance to biotic and abiotic stress — germin-like and/or cupin-domain-containing proteins (20–23) (group C); spherulin-4 domain-containing proteins (24) (group D); concanavalin-A-like lectin protein (25) (group E); chitinase (spot 14) (18); GDSL-like lipase (26–28) (group H); glyoxal oxidases (29) (spots 27 and 31–33); lipocalin (30, 31) (spot 6); and serine proteases from subtilase family (groups I and J) (32, 33)
- metabolism related proteins — ferredoxin-nadp<sup>+</sup> reductase-like protein (19) (group F) and fructose-bisphosphate aldolase (spot 23).

## AN HCP ASSAY FOR PLANT-MADE PHARMACEUTICALS

We demonstrated successful development of a novel HCP assay for biopharmaceuticals derived from the *P. patens* expression host. Further fine tuning of this assay will be necessary before its use in release analytics of DP for clinical trial phase 2. That requires full validation, examination of the HCP population in pre- and postcapture process streams, potential readjustment of the acceptable HCP levels in DP (based on the results from phase 1 clinical trial), and so on.

Through depletion of cross-reactivity between generated capture antibodies and the drug substance

( $\alpha$ Gal), we have also shown that optimization of this newly established “multiproduct” HCP assay to a product-specific assay is feasible. With that, we have accomplished another important milestone for establishment of Greenovation's technology as a next-generation biopharmaceutical production system.

## ACKNOWLEDGMENTS

We thank Dr. Klaus Wölfle (Biomeva GmbH) for help in planning and performing the validation study; Protagen Protein Services GmbH for help in analysis of the HCP antigen mix; and Dr. Claudia Geserick (Biogenes GmbH) for HCP-coverage evaluation analysis. We also thank all Greenovation Biotech GmbH staff for excellent technical assistance.

## REFERENCES

- 1 Eaton LC. Host Cell Contaminant Protein Assay Development for Recombinant Biopharmaceuticals. *J. Chromatogr. A* 705(1) 1995: 105–114.
- 2 Stamm O, et al. Analytical Methods: Host Cell Proteins. *Europ. Biopharmaceut. Rev.* 12, Autumn 2012: 74–80.
- 3 Tscheliessnig AL, et al. Host Cell Protein Analysis in Therapeutic Protein Bioprocessing: Methods and Applications. *Biotechnol. J.* 8(6) 2013: 655–670.
- 4 Wolter T, Richter A. Assays for Controlling Host-Cell Impurities in Biopharmaceuticals. *BioProcess Int.* 3(2) 2005: 40–46.
- 5 Schwertner D, Kirchner M. Are Generic HCP Assays Outdated? *BioProcess Int.* 8(5) 2010: 56–61.
- 6 Wang X, et al. Improved HCP Quantitation By Minimizing Antibody Cross-Reactivity to Target Proteins. *BioProcess Int.* 8(1) 2010: 18–23.
- 7 Shaaltiel Y, et al. *Large Scale Disposable Bioreactor*. WO 2008/135991 A2, 13 November 2008; www.google.com/patents/WO2008135991A2.
- 8 Murray EW, et al. A Host Cell Protein Assay for Biologics Expressed in Plants. *BioProcess Int.* 10(9) 2012: 44–51.
- 9 Decker EL, Parsons J, Reski R. Glyco-Engineering for Biopharmaceutical Production in Moss Bioreactors. *Front. Plant Sci.* 5, 2014: 346.
- 10 Reski R, Parsons J, Decker EL. Moss-Made Pharmaceuticals: From Bench to Bedside. *Plant Biotechnol. J.* 13(8) 2015: 1191–1198.
- 11 Koprivova A, et al. Targeted Knockouts of *Physcomitrella* Lacking Plant-Specific Immunogenic N-Glycans. *Plant Biotechnol. J.* 2(6) 2004: 517–523.
- 12 Reski R, et al. *Transformed Bryophyte Cell Having Disrupted Endogenous Alpha 1,3-Fucosyl and Beta 1,2-Xylosyl Transferase Encoding Nucleotide Sequences for the Production*

of *Heterologous Glycosylated Proteins*. US PTO 7781197 B2. 24 August 2010.

13 Niederkrüger H, Dabrowska-Schlepp P, Schaaf A. Suspension Culture of Plant Cells Under Phototrophic Conditions. *Industrial Scale Suspension Cultures of Living Cells*. Meyer H-P, Schmidhalter D, Eds. Wiley-Blackwell VCH: Berlin, Germany, 2014.

14 Große T, Niederkrüger H, Schaaf A. *Filtration of Cell Culture Supernatants*. WO 2014013045 A1, 22 January 2014; www.google.com/patents/WO2014013045.

15 Thalhamer J, Freund J. Cascade Immunization: A Method of Obtaining Polyspecific Antisera Against Crude Fractions of Antigens. *J. Immunol. Meth.* 66(2) 1984: 245–251.

16 Shen J-S, et al. Mannose Receptor-Mediated Delivery of Moss-Made  $\alpha$ -Galactosidase A Efficiently Corrects Enzyme Deficiency in Fabry Mice. *J. Inherit. Metab. Dis.* 27 August 2015: 1–11; doi:10.1007/s10545-015-9886-9.

17 Zimmer AD, et al. Reannotation and Extended Community Resources for the Genome of the Non-Seed Plant *Physcomitrella patens* Provide Insights into the Evolution of Plant Gene Structures and Functions. *BMC Genomics* 14, 2013: 498.

18 Tintelnot S. *Der Einfluss von Abscisinsäure auf die Pflanzliche Zellwand: Untersuchung Extrazellulärer Proteine beim Laubmoos Physcomitrella patens* (PhD thesis). Universität Freiburg: Freiburg, Germany, 2006.

19 Lehtonen MT, et al. Protein Secretome of Moss Plants (*Physcomitrella patens*) with Emphasis on Changes Induced By a Fungal Elicitor. *J. Proteome Res.* 13(2) 2014: 447–459.

20 Lane BG, et al. Homologies Between Members of the Germin Gene Family in Hexaploid Wheat and Similarities Between These Wheat Germins and Certain *Physarum spherulins*. *J. Biol. Chem.* 266(16) 1991: 10461–10469.

21 Lane BG. Oxalate, Germins, and Higher-Plant Pathogens. *IUBMB Life* 53(2) 2002: 67–75.

22 Dunwell JM, et al. Germin and Germin-Like Proteins: Evolution, Structure, and Function. *Crit. Rev. Plant Sci.* 27(5) 2008: 342–375.

23 Zhang Z, Collinge DB, Thordal-Christensen H. Germin-Like Oxalate Oxidase, a H<sub>2</sub>O<sub>2</sub>-Producing Enzyme, Accumulates in Barley Attacked by the Powdery Mildew Fungus. *Plant J.* 8(1) 1995: 139–145.

24 Cuming AC, et al. Microarray Analysis of Transcriptional Responses to Abscisic Acid and Osmotic, Salt, and Drought Stress in the Moss, *Physcomitrella patens*. *New Phytol.* 176(2) 2007: 275–287.

25 De Hoff PL, Brill LM, Hirsch AM. Plant Lectins: The Ties That Bind in Root Symbiosis and Plant Defense. *Mol. Genet. Genomics* 282(1) 2009: 1–15.

26 Oh IS, et al. Secretome Analysis Reveals an Arabidopsis Lipase Involved in Defense Against *Alternaria brassicicola*. *Plant Cell Online* 17(10) 2005: 2832–2847.

27 Naranjo MA, et al. Overexpression of *Arabidopsis thaliana* LTL1, a Salt-Induced Gene Encoding a GDSL-Motif Lipase, Increases Salt Tolerance in Yeast and Transgenic Plants. *Plant Cell Environ.* 29(10) 2006: 1890–1900.

28 Hong JK, et al. Function of a Novel GDSL-Type Pepper Lipase Gene, CaGLIP1, in Disease Susceptibility and Abiotic Stress Tolerance. *Planta* 227(3) 2008: 539–558.

29 Guan X, et al. Transient Expression of Glyoxal Oxidase from the Chinese Wild Grape *Vitis pseudoreticulata* Can Suppress Powdery Mildew in a Susceptible Genotype. *Protoplasma* 248(2) 2011: 415–423.

30 Charron J-BF, et al. Identification, Expression, and Evolutionary Analyses of Plant Lipocalins. *Plant Physiol.* 139(4) 2005: 2017–2028.

31 Wang X, et al. Proteomic Analysis of the Response to High-Salinity Stress in *Physcomitrella patens*. *Planta* 228(1) 2008: 167–177.

32 Schaller A. A Cut Above the Rest: The Regulatory Function of Plant Proteases. *Planta* 220(2) 2004: 183–197.

33 Wolf S, Rausch T, Greiner S. The N-terminal Pro Region Mediates Retention of Unprocessed Type-I PME in the Golgi Apparatus. *Plant J. Cell Mol. Biol.* 58(3) 2009: 361–375. 🌐

Corresponding author **Paulina Dabrowska-Schlepp** is analytics team leader, **Mathias Knappenberger** was at the time this project started downstream processing team leader, **Holger Niederkrüger** is head of production, and **Andreas Schaaf** is chief scientific officer at Greenovation Biotech GmbH, Hans-Bunte Straße 19, D-79108 Freiburg, Germany; pdabrowska@greenovation.com. **Stefan Sommerschuh** is head of assay development, and **Nicole Gliese** is project manager at BioGenes GmbH, Köpenicker Straße 325, D-12555, Berlin, Germany.

For reprints, contact Rhonda Brown of Foster Printing Service, rhondab@fosterprinting.com, 1-866-879-9144 x194.

## Continued from page 31

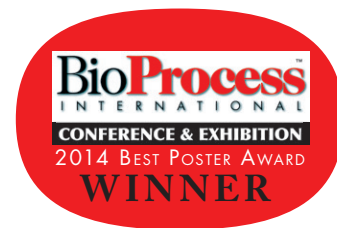
18 Peiris KJ, et al. Development of Residual Host-Cell Protein Assays for Recombinant Microbial Biopharmaceuticals. 5th Annual European Gyrolab Seminar: Siena, Italy, 2011.

19 Ramsbramaniam N. Rapid Process Development Enabled By Automated, Single Use High-Throughput Technologies. Annual Meeting of the Society for Industrial Microbiology and Biotechnology: Philadelphia, PA, 2015.

20 Roussis M. Automated Quantification of Residual protein A Ligands with Gyrolab Protein A Kit (poster). BioProcess International Conference and Exhibition: Boston, MA, October 2015.

21 Lehtonen P, Inganas M. *Quantification of MabSelect SuRe Ligand in Presence of Excess Amounts of IgG on Gyrolab*. Gyros AB: Uppsala, Sweden, 2009; www.gyros.com/why-gyros/knowledge-center/references/#impurity.

22 Wang L, et al. *Product Quantification (IgG Titer) Using an Automated Analytical Platform — Gyrolab Workstation*. Gyros AB: Uppsala, Sweden, 2014; www.gyros.com/why-gyros/knowledge-center/downloads. 🌐



**Eike Zimmermann**, PhD, is an associate director; **Lin Wang**, PhD, is a scientist II; **Anoushka Durve** is manager of analytical science; and **Kenji Furuya**, PhD, is department head of analytical science at Boehringer Ingelheim, 6701 Kaiser Dr, Fremont, CA 94555; 1-510-284-6252; eike.zimmermann@boehringer-ingelheim.com. Formerly a member of the BI team, **Fang Li** is now a QC specialist at Bayer HealthCare Pharmaceutical, Inc. Formerly a senior associate scientist with the BI team, **Li Zhang** is now associated director at LakePharma.

For reprints, contact Rhonda Brown of Foster Printing Service, rhondab@fosterprinting.com, 1-866-879-9144 x194.